International Journal of Engineering Research and General Science Volume 2, Issue 5, August-September, 2014
ISSN 2091-2730

Determination of Distortion Developed During TIG welding of low carbon steel plate

Atma Raj M.R, Joy Varghese V.M.
Mechanical Engineering Department
SCT College of Engineering
Thiruvananthapuram, Kerala, India
atmarajmr@gmail.com

Abstract—TIG welding is widely used in modern manufacturing industries. In almost all kinds of metals, TIG welding produces high quality welds. Determination of distortions developed during welding is one of the major goals of welding simulation.Predictions of distortions are necessary to maintain the design accuracy of critically welded components in the design stage itself rather than doing corrective measures after welding. The purpose of present work is to predict the distortion developed during TIG welding of low carbon steel plate. In this study, 3-D FE model is developed to analyze the distortion during TIG Welding of steel plate. In numerical analysis thermal and structural analysis were carried out sequentially. The thermal loads are the main input of structural analysis. For the analysis the effect of distortion in different plates were calculated and compared to get the plane of maximum distortion. An experiment was conducted to measure the distortion or deformation in a welded plate.

Keywords—TIG, Distortion or Deformation, welding modeling, CMM, FEM, Discretization, welding heat source.

INTRODUCTION

Tungsten inert gas welding, TIG is widely applied in manufacturing process for different types of materials like Aluminum, Mild steel and different type of stainless steel alloy grades. The optimization of TIG welding process parameters play important role for the final product quality in terms of weld distortions, joint efficiency and mechanical properties. As welding process involves the heating and cooling process in non-uniform manner, the distortions are unavoidable. The weld contributes to the development of several kinds of distortions like longitudinal, transverse or angular distortions [1]. Distortion in welding is due to non-uniform heating and cooling produced during welding. Controlling distortion is very important as it severely affects the dimensional tolerance limits. Correcting distortion is costly and in many cases not possible. So it is necessary to establish a procedure that minimizes distortion and establish rational standards for acceptable limits for distortion. Arc welding involves intense local heating of the weld region and conduction of this heat in to the surrounding material. However this expansion is constrained by the cooler material surrounding it, leads to plastic deformationof hotter material. Reducing and controlling distortion requires the fundamental knowledge of residual stress and other factors which cause distortion. During welding and subsequent cooling, thermally induced shrinkage strains build up in the weld metal and the base metal regions. The stresses resulting from these shrinkage strains combine and react to produce bending, buckling etc.

LITERATURE REVIEW

The welding heat source was assumed to be a point and line source in the early stages of welding modeling. During the initial stages of welding heat transfer modeling conduction based models were developed and later convection models were developed which are found to be more accurate especially in and around the weld pool According to D. Kolbcar [2], Rosenthal developed a relation for both line and point moving sources at first. In 1969 Pavelic introduced Gaussian form of distribution which is used by many researches and has been using the same because of its simplicity and accuracy of such an assumption. This model is not suitable for modeling an inclined welding torch. Goldak et al [3] in 1984 introduced double ellipsoidal distribution which is the most suitable distribution for a stationary welding source and can account for the inclined torch position,this model also fails for moving torches.

As an extension of this work in 2003 Sapabathy et al introduced double ellipsoidal model with a differential distribution at the front and back portion of arc which is most suitable for even vibrating heat sources, that can be used for modeling any type of welding technique including wave technique. A new method for calculating the thermal cycles in the heat affected zone during gas metal arc (GMA) welding was done by M.A. Wahab et al [4] and the thermal cycles were predicted in order to estimate the depth of weld

penetration, the geometry of the weld pool and the cooling rates. They concluded that to obtain optimal weld pool geometry for tungsten inert gas (TIG) welding the selection of process parameters such as front height, front width, back height and back width of the weld pool play an important role. The finite element distortion analysis in two dissimilar stainless steel welded plate is analyzed by J.J. del Coz Díaz et.al. [5].They studied the effect of TIG welding in duplex stainless steels. In order to predict the welding deformation in fillet welds, Dean Deng et.al. [6] developed a 3D thermal elastic plastic finite element computational procedure and validated numerical results with the experimental measurements and he concluded that numerical models can be effectively used for the prediction of welding distortion.

1. EXPERIMENTAL DETERMINATION FOR PREDICTING DISTORTION

The experiment was conducted for finding out the distortion of welded plate after TIG welding. A numerical analysis is carried out and the results were compared with the experimental results

Experimental procedure

In the present work, MS specimens of dimensions 150mm X 50x6 mm were considered. The base plate material used was commercial mild steel. Each specimen were filed using a flat file and all the surfaces were grinded with surface grinding machine of 240 grit. Flexible abrasive paper (silicon carbide) was used to remove all impurities and to get the required surface finishThe co-ordinates of the drilled hole were measured using co-ordinate measuring machine (CMM).Two of the side surfaces (at weld start point) are set as the reference planes and the intersection point of the two reference planes is set as the reference point. With reference to these reference points the centre of the holes were determined by measuring the cylindrical surface of the holes .Hence all the co-ordinates of the four holes were determined.

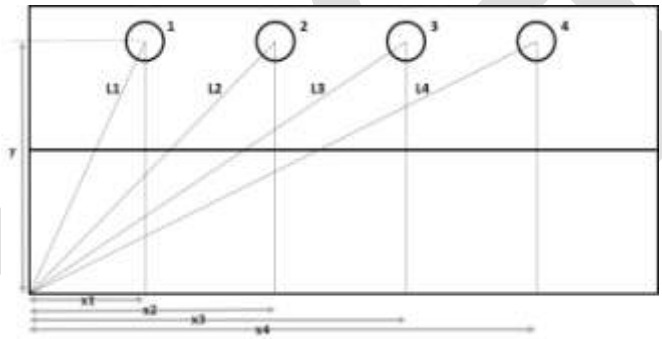

Fig.1 Schematic representation of specimen for distortion measurement in CMM

Four holes of 2mm diameter were drilled at position as in Fig 1. The measurements and the results were saved on a spread sheet. Then welding was carried out on plates by applying on TIG welding torch to get a bead on the plate in which the torch travelled at a constant speed of 2mm/sec. Single-pass; autogenous, bead-on-plate TIG welds were made along the center line of the test specimens. A torch with a standard 2% thoriated tungsten electrode rod with a 3.2 mm diameter was used.The electrode tip was a blunt point with a 45° angle. Argon gas of 99.99% purity was used as the shielding gas. The tip angle of the electrode was grounded, and the electrode gap was measured for each new weld prior to welding to ensure that the welding was performed under the same operating conditions. After welding, test specimens are cleaned and the co-ordinates of the welded specimen were measured using CMM with respect to the same reference before welding. The results were recorded on spreadsheet document. Measurements taken before and after welding were compared. Distortions at specified points were determined by the difference between the readings taken before and after welding.

Fig.2. Accurate-Spectra Coordinate Measuring Machine

Fig 1 shows the schematic diagram of distortion measurement process and Fig.2. shows the Accurate Spectra Coordinate Measuring Machine which is used for measuring the distortion in specimen.The TIG welding process was performedon the test specimenusing TIG welding machine (WARPP–TIME, WSM- 160). Table-1 lists the welding conditions used in this study.

Table.12: Welding parameters for TIG welding experiments.

Specifications	**values**
Diameter of electrode	0.8mm
Tip angle of electrode	60◦
Electrode gap	3mm
Shielding gas	Argon
Gas flow rate	25 L/min
Welding current	150A

2. FINITE ELEMENT ANALYSIS

The finite element analysis is carried out to analyze the thermal cycles and nature of residual stressfor a TIG welding in a low carbon steel plate. The dimensional changes during welding are negligible and mechanical work done is insignificant compared to thermal energy from the welding arc. The thermo-mechanical behavior of weldment during welding is simulated using uncoupled formulation. Thermal problem is solved independently from the mechanical problem to obtain thermal cycles.

A. Thermal Analysis

Analysis is done for a plate of 150mm length and 50mm width of 6mm thickness fig.3. Because of symmetry one half of the model is selected for the analysis.

Fig.3. 17D Finite Element model.

Fig 2 shows the 3D finite element model which is used for thermal analysis. The model is discretized to finite number of elements as shown. The element type used for thermal analysis is 20 nodded thermal brick elements as shown in fig 2.The thermal physical properties [7] and mechanical properties [8] of the low carbon steel are obtained from the available literature.

The governing equation for welding transient heat transfer is given by

$$\rho c \frac{\partial T}{\partial t}(x,y,z,t) = -\nabla . q(x,y,z,t) + Q(x,y,z,t) \qquad (1)$$

where ρ is the density of the materials, c is the specific heat capacity, T is the current temperature, q is the heat flux vector, Q is the internal heat generation rate, x, y and z are the coordinates in the reference system, t is the time, and ∇ is the spatial gradient operator.

In this study, the heat from the moving welding arc is applied as a volumetric heat source with a double ellipsoidal distribution proposed by Goldak et al. [1], and is expressed by the following equations:

$$q(x,y,z,t) = \frac{f_r \eta U I 6\sqrt{3}}{abc_r \pi \sqrt{\pi}} exp\left[-3\left(\frac{y}{a}\right)^2 - 3\left(\frac{z}{b}\right)^2 - 3\left(\frac{x+v(\tau-t)}{c_r}\right)^2\right]$$

(2)

Where x, y and z are the local coordinates of the double ellipsoid model. f is the fraction of heat deposited in the weld region. U and I are the applied voltage and current. The arc efficiency η, is assumed to be 70% for the TIG welding process. The parameters a, b and c are related to the characteristics of the welding heat source. The parameters of the heat source can be adjusted to create a desired melted zone according to the welding conditions. A function is generated using ANSYS APDL code to apply the heat generation to the plates.

To consider the heat losses, both the thermal radiation and heat transfer on the weld surface are assumed. Radiation losses are dominating for higher temperatures near and in the weld zone, and convection losses for lower temperatures away from the weld zone. To accommodate these both effects combined temperature-dependent heat transfer coefficient is applied on boundaries.

$$h = 24.1 \times 10^{-4} \times \varepsilon \times T^{1.61} \quad (3)$$

Where ε is the emissivity of the body surface which is taken as 0.8, T is the temperature of the material surface. The above thermal boundary condition is employed for all free boundaries of the plates. The thermal effects due to solidification of the weld pool are modeled by taking into account of solidus temperature as1415˚C, liquidus temperature as 1477˚C and the latent heat of fusion as 285000kJ/kg.

B. Mechanical Analysis

The same discretized thermal model is used for Mechanical analysis. Here the element type is changed to the 20 noded brick element with degree of freedom. The temperature histories of each node from the preceding thermal analysis are input as nodal body load in conjunction with temperature-dependent mechanical properties and structural boundary conditions. During the welding process, solid-state phase transformation does not occur in the base metal, and in the weld metal, the total strain rate can be decomposed into three.

$$\epsilon_{total} = \epsilon_e + \epsilon_P + \epsilon_{th} \quad (3)$$

ϵ_{total} is the total strain produced, ϵ_e is the elastic strain, ϵ_p is the plastic strain and ϵ_{th} is the thermal strain

3. RESULTS AND DISCUSSION

In order to study the effect of distortion on plates, the FE analysis is carried out using the parameters given in Table 1

Table.2: Weld parameters

V	I (A)	Weld pool parameters			υ mm/s	H (%)
12	150	a(mm) 4	b(mm) 3	c(mm) 5	2	0.7

Fig.4.shows the various weld pool parameters, in a double ellipsoidal distribution proposed by Goldak et al. [1],

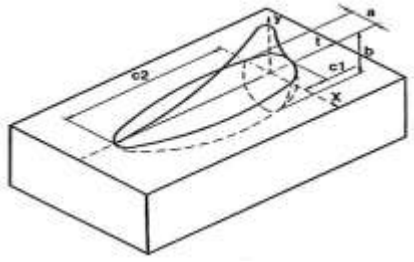

Fig.4. Weld pool parameters[2]

4. Prediction of maximum distorted plane during welding of plates

Finite element analysis is carried out to study the maximum distorted dimension of the specimen.For the analysis the deformations were defined parallel and perpendicular to the weld line at each of the distances near and away from the weld line and the corresponding X, Y, Z distortions were obtained through the analysis to determine the maximum distorted plane and direction during welding of plates. For that distortion along X, Y, and Z direction were plotted at different locations over the plate.Fig.4. Shows the X direction distortion along a line (AB) at the top, middle and bottom surface of the plate.Fig.5.shows Y direction distortion along a line (AB) at the top, middle and bottom surface of the plate.Fig.6.shows Z direction distortion along a line (AB) at the top, middle and bottom surface of the plate.

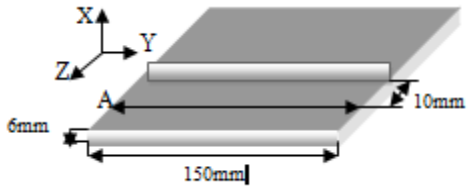

Fig.5.X, Y, Z Distortion along a line parallel to the weld at a distance of 10mm

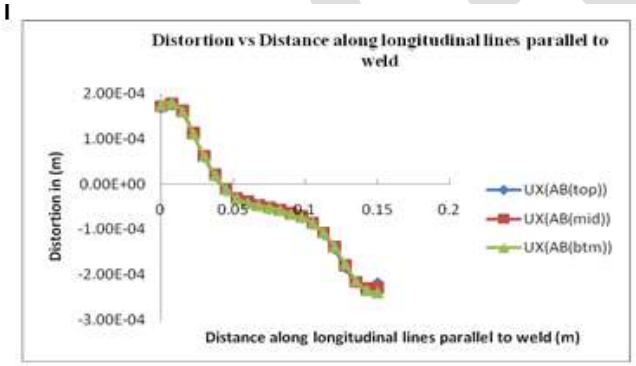

Fig.6. X direction distortion along lines parallel to weld at top, middle and bottom surface

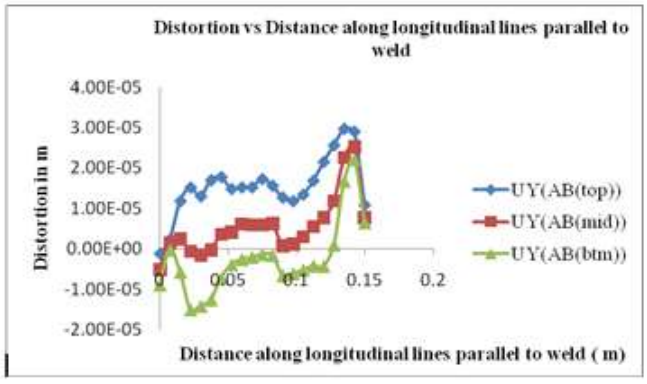

Fig.7.Y direction distortion along lines parallel to weld at top, middle and bottom surface

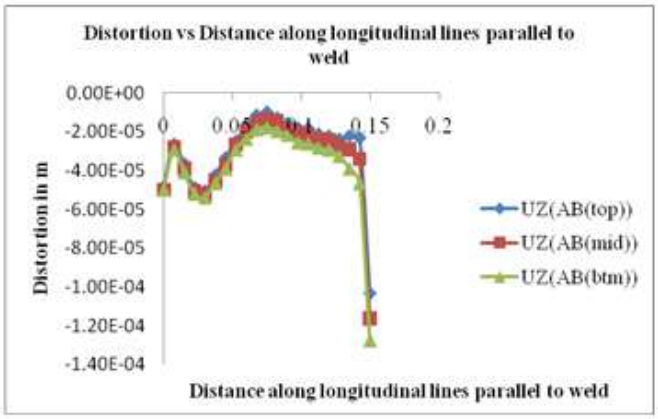

Fig.8.Z direction distortion along lines parallel to weld at top, middle and bottom surface.

On comparing the distortion along X, Y and Z directions, it can be observed that maximum distortion has occurred in the bottom surface of the plate. So analysis in bottom surface will be considered in future study. Similarly certain lines perpendicular to the weld line has also been analyzed to find the maximum distorted surface of the plate. The graphs shown below gives the X, Y and Z direction distortions for a line at the top, middle and bottom surface of the plate.

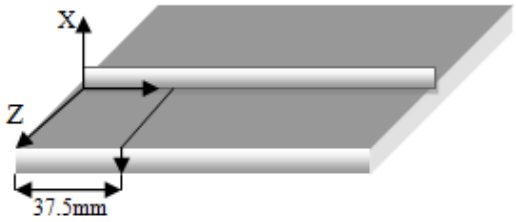

Fig.9. X, Y, Z Distortion along a line perpendicular to the weld at a certain distance from weld

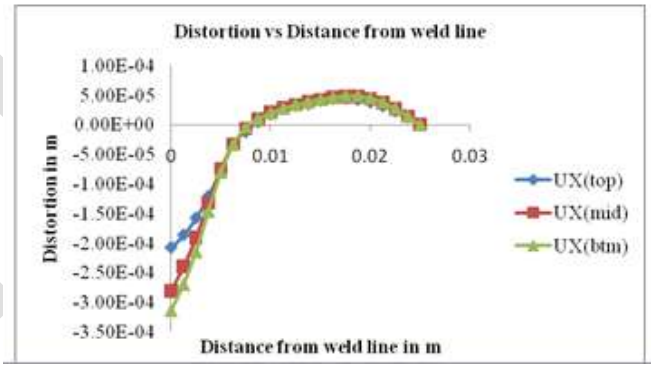

Fig.10. X direction distortion along lines perpendicular to weld line at a distance of 37.5 mm from edge

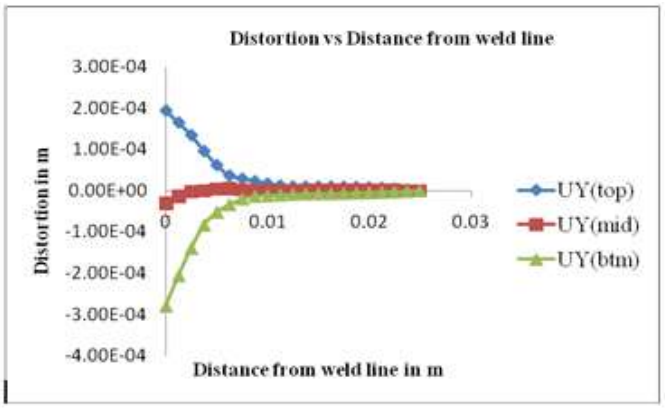

Fig.11. Y direction distortion along lines perpendicular to weld line at a distance of 37.5 mm from edge

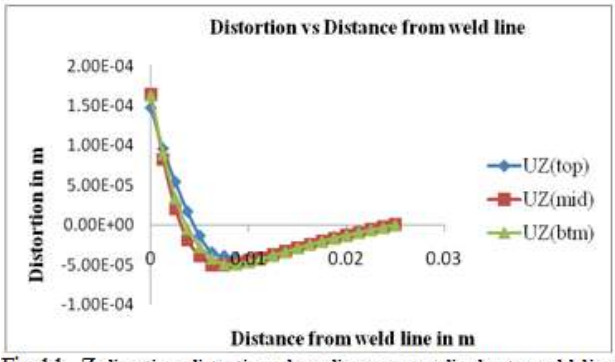

Fig.11. Z direction distortion along lines perpendicular to weld line at a distance of 37.5 mm from edge

5. Comparison of distortion in different directions on bottom surface(parallel to the weld line)

The specimen shown below is of dimension 150x50x6mm.The shaded region represents the welded area. A line 10 mm away from the weld at the bottom surface is considered for the analysis.

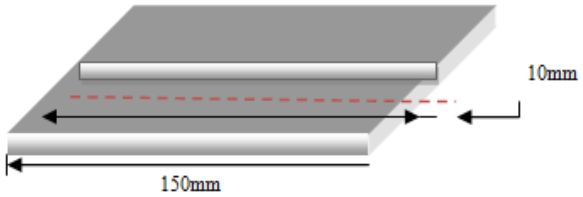

Fig.13. Distortion in different directions along a line at the bottom surface

On comparison of distortion along X, Y and Z direction it is clear that the bottom surface shows the maximum distortion. Hence another analysis has been carried out to determine among X, Y and Z direction, which direction shows the maximum distortion on the bottom surface. For that a line at a certain distance away and parallel to the weld were considered.

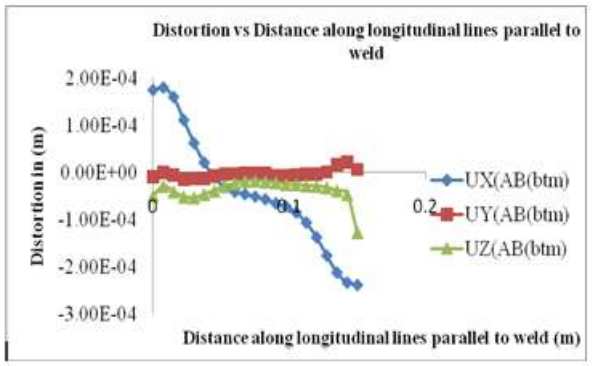

Fig.14. Distortion in X, Y and Z directions along a line at the bottom surface of the plate (parallel to weld line)

From the graph it can be concluded that at the bottom surface, X direction shows the maximum distortion and the other two directions shows comparatively minimum value. To verify the result a line perpendicular to the weld has also been analyzed.

6. Comparison of distortion in different directions on bottom surface(perpendicular to the weld line)

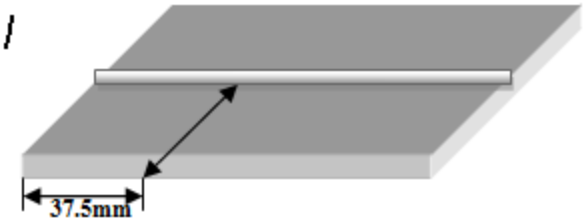

Fig.15.Distortion in different directions along a line perpendicular to the weld

For the analysis a line perpendicular to the weld at a distance of 37.5 mm were considered. Finite element analysis has been carried out to study the maximum distorted dimension of the plate in the bottom surface. Fig.15. Shows the distortion in X, Y and Z directions along a line perpendicular to the weld at the bottom surface of the plate On comparing the distortion along X,Y&Z directions, maximum distortion has occurred along the weld direction i.e. along X direction, while other direction shows comparatively less deformation. So here analysis in X direction will be considered in future study.

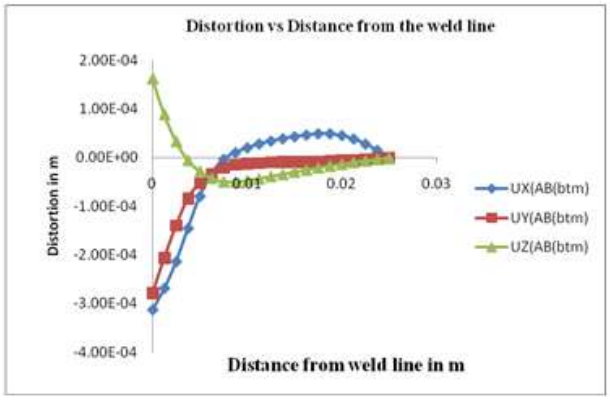

Fig.16. Distortion in X, Y and Z directions along a line at the bottom surface of the plate (perpendicular to weld line)

From the Fig.16 also it can be concluded that X direction has the maximum distortion than Y and Z direction.

7. Comparison of X distortion along lines parallel to weld directions on bottom surface

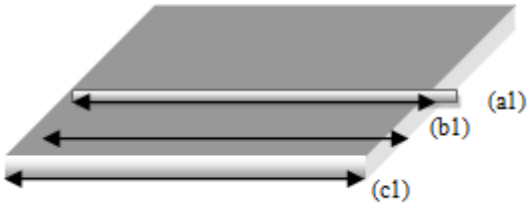

Fig.17.X direction distortion along different lines parallel to the weld

An analysis has been carried out to determine the deformation pattern along the weld line and at a distance 10 mm away from the weld line. a1 represents the weld line, b1 at a distance of 10mm from the weld line and c1 at a distance of 25mm from the weld line on the bottom surface of the plate. From the analysis the weld line shows the maximum distortion and the rate of distortion goes on decreasing away from the weld line.

8. Variation in distortion parallel to the weld line at a certain distance away from the weld line

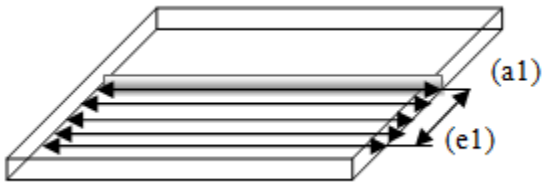

Fig.18.Distortion along different longitudinal lines parallel to weld

In order to find whether there is any critical variation in distortion pattern in between the weld line and at a line 10 mm away from the weld line four nearby points were taken from the weld line and the deformation plots were obtained parallel to the weld line at each of the distances. From the analysis it is clear that there is no shift in the distortion pattern and it is varying uniformly between the centre line and the line which is 10 mm away from the weld line.

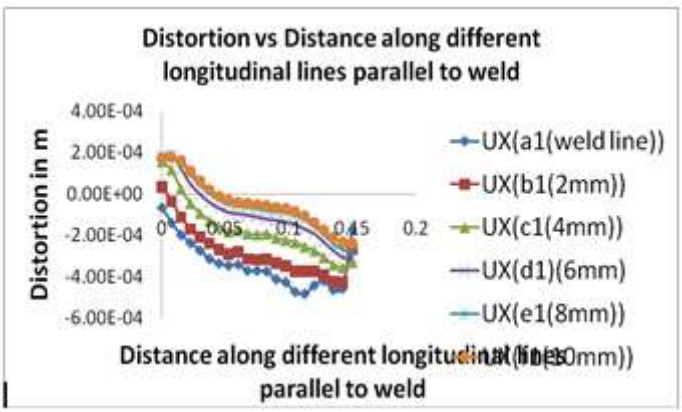

Fig.19.X direction distortion along different longitudinal lines parallel to weld on bottom surface

9. Comparison of X distortion along line perpendicular to weld on bottom surface

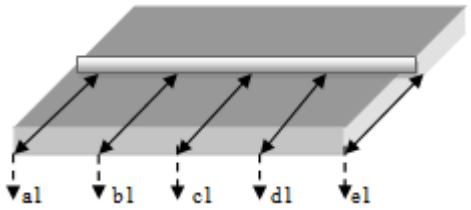

Fig.20.X direction distortion along different lines perpendicular to the weld

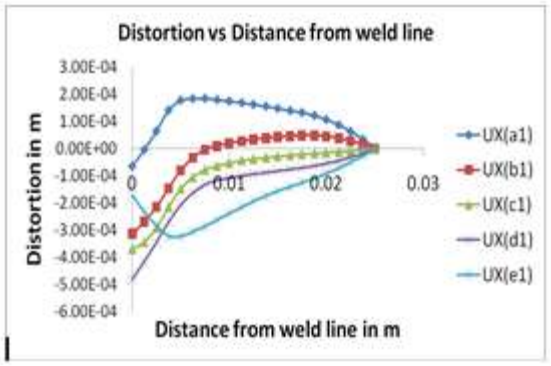

Fig.21.Distortion along lines perpendicular to the weld in X direction on bottom surface

An analysis has been carried out to determine the deformation pattern along certain lines perpendicular to the weld. From the analysis it is clear that the higher heat input leads to prone distortion. At the initial point of weld the nature of distortion is positive and near the end region where the weld ends shows the maximum distortion due to higher heat input.

10. Comparison of Experimental and Numerical Result for 6mm Plate

Hole no	Numerical Result	Experimental Result
1	.016	.03
2	.022	.02
3	.021	.03
4	.023	.01

Table.4: Numerical and Experimental results

Conclusion

The effect of distortion on welding of low carbon steel plates has been studied. The primary results and conclusions can be summarized as follows:

1. During TIG welding of steel plates the surface opposite to the weld shows maximum distortion.

2. Among the three directions X, Y, Z directions, X direction (along the weld) shows maximum distortion while others shows comparatively less.

3. On comparing the distortion pattern in and around the weld pool, the maximum distortion has occurred near the weld and the rate of distortion goes on decreasing as the distance from the weld increases.

4. The numerical and experimental results are validated.

REFERENCES:

[1]. K. Masubuchi, Control of Distortion and Shrinkage in Welding, Bulletin of WRC; 149.Materials Science, Vol. 31, 2004, pp. 368–378

[2]. D. Klobcar, J. Tu_sek and B. Taljat: "Finite element modeling of GTA weld surfacing applied to hot-work tooling,"Computational

[3]. John Goldak, AdityaChakravarti and Malcolm Bibby:" A new finite element model for welding heat sources, "Metallurgical Transactions B 15, June-1984, pp. 299–305.

[4]. S.W. Shyu, H.Y. Huang, K.H. Tseng, and C.P. Chou, 2008,"Study of the Performance of Stainless Steel A- TIG Welds", ASM International JMEPEG vol.17(2),pp 193–201.

[5]. M.A. Wahab, M.J. Painter and M.H. Davies:"The prediction of the temperature distribution and weld pool geometry in the gas metal arc welding process", Journal of Materials Processing Technology, Vol. 77, 1998, pp. 233–239

[6]. DeanDeng,WeiLiang,HidekazuMurakawa,"Determination of welding deformation in fillet-welded joint by means of numerical simulation and comparison with experimental measurements", Journal of Materials Processing Technology 183 (2007) 219–225.

[7]. Talijat,B.,Radhakrishnan,B.,Zacharia,T.,"Numerical Analysis of GTA welding process with emphasis on post-soldification phase transformation effects on residual stress".J.Mater.Sci Eng. A 246,1998,pp 45-44

[8]. Afzaal M.Malik,Ejaz.M Qureshi,Naeem Ullah Dar,Iqbal Khan,"Analysis of circumferentially arc welded thin-walled cylinders to investigate the residual stress fields.",J.Thin-Walled Structures-46,2008pp1391-1401.

[9]. G.W. Krutz, L.J. Segerlind, Finite element analysis of welded structures, Welding Journal Research Supplement 57 (1978) 211s–216